NUMERICAL STUDY OF SIDEWALL FILLING FOR GAS-FED PULSE DETONATION ENGINES

by

WUNNARAT RONGRAT

Presented to the Faculty of the Graduate School of
The University of Texas at Arlington in Partial Fulfillment
of the Requirements
for the Degree of

DOCTOR OF PHILOSOPHY

THE UNIVERSITY OF TEXAS AT ARLINGTON

December 2012

This thesis is dedicated to my grandmother who taught me that the most valuable thing of this world is knowledge and who supported me in every way.
It is also dedicated to the Royal Thai Air Force for giving me a great opportunity to pursue my master degree at University of Texas at Arlington.

ACKNOWLEDGEMENTS

First of all, I would like to thank Dr. Frank K. Lu, my advisor, who motivated and always stimulated me to proceed with this research by his significant suggestions. I made the right decision to work with him which increased my knowledge of computational fluid dynamics. I want to record my appreciation to Dr. Wilson, the Aerospace Engineering Graduate Advisor, who gave me many suggestions since I began my graduate studies and also to Dr. Tong who showed interest in my topic to be a member of my thesis committee. Moreover, my opportunity to pursue the master degree at University of Texas at Arlington will be impossible without financial support from the Royal Thai Air Force.

November 7, 2012

ABSTRACT

NUMERICAL STUDY OF SIDEWALL FILLING FOR
GAS-FED PULSE DETONATION ENGINES

WUNNARAT RONGRAT, Ph.D.

The University of Texas at Arlington, 2012

Supervising Professor: Frank K. Lu

Pulse detonation engines for aerospace propulsion are required to operate at 50–100 Hz meaning that each pulse is 10–20 ms long. Filling of the engine and the related purging process become dominant due to their long duration compared to ignition and detonation wave propagation. This study uses ANSYS FLUENT to investigate the filling of a 1 m long tube with an internal diameter of 100 mm. Six different configurations were investigated with an endwall port and various sidewall arrangements, including stagger and inclination. A stoichiometric mixture of gaseous octane and air at STP was used to fill the tube at injection rates of 40, 150 and 250 m/s. Phase injection was also investigated and it showed performance improvements such as reduced filling time and reduced propellant escape from the exit.

TABLE OF CONTENTS

LIST OF ILLUSTRATIONS

LIST OF TABLES

CHAPTER 1

INTRODUCTION

1.1 Pulse Detonation Engine

Pulse detonation engines (PDEs) have been widely studied for many years. These engines are proposed for different aerospace platforms as potential replacements for turbomachinery-based engines. Detonation-based engine research has shown potential benefits such as better theoretical performance[1] compared to traditional deflagration-based engines [2, 3]. PDEs have been proposed to operate from subsonic speeds to about Mach 5. The simplicity in design also facilitates manufacturing and maintenance.

1.1.1 Detonation Engine Operation Cycle

Basically, a PDE consists of a tube which is closed at one end and opened at the other for exhausting the combustion products. As shown in Fig. 1.1, the intermittent operation of a PDE can be divided into seven processes. Beginning at the top of the figure is the end of the purging stage with the detonation tube at ambient conditions. The second step is filling where a stoichiometric mixture of fuel and air is injected into detonation tube through an injection port at the closed end on the left. The fill time of the reactants is t_{fill}. The third step is the ignition or initiation stage whose duration is t_{int}. The next two stages where the detonation wave propagates through the tube and arrives at the closed end takes a time of t_{det}. After that, thrust is generated from the exhaust. Finally fresh air is introduced to purge the combustion products and to cool the tube, preparing for the next cycle. For simplicity, the thrust

and purge stages are considered together whose duration is t_{purg} that is approximately equal to the fill time. Therefore, the total cycle time can be written as

$$t_{cycle} = t_{fill} + t_{int} + t_{det} + t_{purg} \tag{1.1}$$

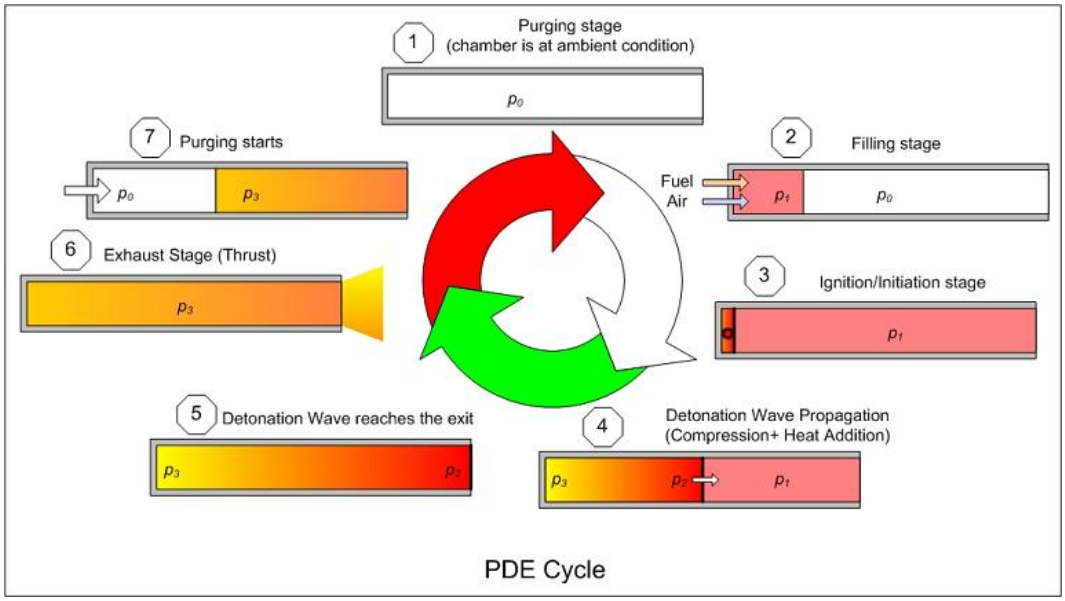

Figure 1.1 Schematic of the stages of a detonation engine cycle.

The ignition and detonation propagation times are a fraction of a millisecond which can be ignored compared to the fill and purge times. Studies have shown that PDEs for aerospace applications should be operated around 50–100 Hz. This means that t_{cycle} = 10–20 ms. This critical time requirement is the subject of the present study, focusing on different strategies for decreasing the fill time. As a representative problem using vaporized hydrocarbons and air, a 1 m long detonation tube with 100 mm internal diameter is the chosen geometry. These dimensions allow sufficient distance for deflagration-to-detonation transition and for ensuring that detonation cells can form[4, 5].

1.2 Research Objectives

A numerical study performed by ANSYS FLUENT was used to examine filling of a detonation tube by gaseous propellants. Various filling strategies and conditions were investigated in this study to fulfill the following objectives:

- Determine the performance of different configurations at different injection rates
- Change the strategy by phase injection for candidate cases which give high performance by parallel injection

Six cases were studied to satisfy the objectives. The first utilizes only an injection port at the closed end, this forming the reference, baseline case. The other cases all have the same endwall injection but with extra ports on the side, namely opposing sidewall, staggered sidewall, opposing "showerhead" and opposing angled injection (downstream and upstream angle).

CHAPTER 2

NUMERICAL MODELING

2.1 Case Studies

For study CFD analysis, ANSYS Workbench was used for CFD analysis. In this study, as shown in Fig 2.1 all three-dimensional models were created by ANSYS DESIGN MODELER. ANSYS MESHING automatically imported the thre-dimensional CAD geometry from DESIGN MODELER, defining a tetrahedral unstructured mesh and the type of boundary conditions. Numerical analysis was then performed using ANSYS FLUENT with post-processing by ANSYS CFD-Post.

2.1.1 Modeling

The configurations that were investigated were in most part based on a one meter long and 50 mm radius tube with 10 mm radius circular injection ports. The six case studies that were studied are as follows:

- Case 1: This has a single end-wall port which is baseline configuration as shown in Fig. 2.2. The single injection port is located at the closed end of tube which injected the premixed gaseous propellants into the tube. While the other side

Figure 2.1 Numerical Method Solver Flow Chart.

of tube is a 100 mm diameter outlet for exhausting the products in an actual engines.

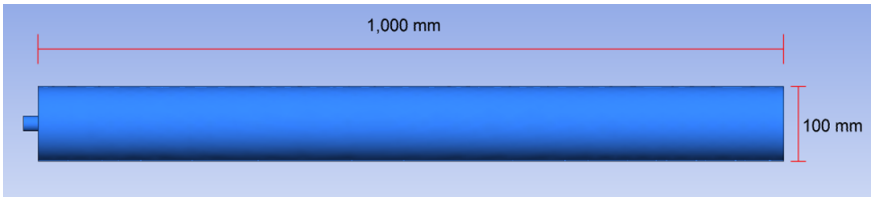

Figure 2.2 Case 1: Single end-wall port.

- Case 2: This consists of a single end-wall port and an array of four pairs of opposing sidewall ports all with the same circular opening of 10 mm radius. The sidewall ports are located at 150, 350 and 550 mm from the closed end as shown as Fig. 2.3. This sidewall injection concept was introduced to (i) increase the flow rate with nine ports of the same size thereby speeding up the fill and (ii) to reduce dead regions around the closed end of the tube.

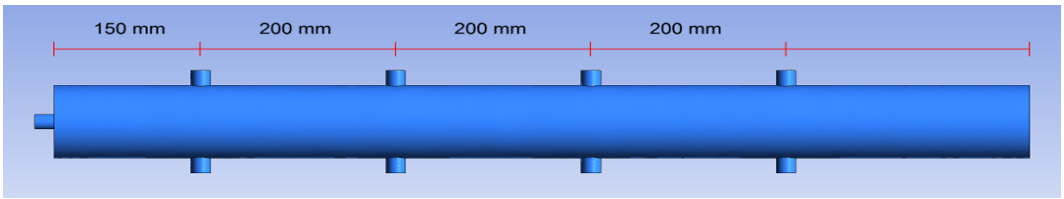

Figure 2.3 Case 2: Single end-wall port and an array of four pairs of opposing.

- Case 3: This is similar to Case 2 but with the sidewall ports shifted alternately by 200 mm as shown in Fig. 2.4. This configuration was also thought to be capable of speeding up the fill and possibly reducing dead regions caused by opposing jets.

- Case 4: This is similar to Case 2 but the single port at each sidewall location is replaced by a cluster of four smaller sized, identical ports with a 5 mm radius known as a "showerhead." This configuration was thought to be able to spread the propellant over a wider region compared to a single port.
- Case 5: Sidewall injection with ports inclined downstream (45 deg) also based on Case 2. This configuration is thought to be able to fill the tube rapidly by reducing blockage due to 90 deg injection.
- Case 6: This is similar to Case 5 but with the injection ports pointing upstream at 45 deg. This configuration is also thought to be able to speed up the fill by reducing blockage due to the filling process itself, to reduce dead regions and to prevent waste.

2.1.2 Meshing

ANSYS MESHING generated a computational mesh throughout the flow volume for CFD analysis. A fine tetrahedral mesh was generated at the edges in order to resolve the complicated gradients expected at those locations. The smallest and largest element sizes were 0.5 and 10 mm respectively. Figures 2.8 and 2.9 illustrate the mesh distribution for Cases 4 and 6 respectively. The final pre-processing in MESHING was to assign boundary conditions at the walls, inlets, the symmetry plane and the outlet.

Table 2.1 Meshing summary

Case	**1**	**2**	**3**	**4**	**5**	**6**
Nodes	15852	37676	37523	157199	50091	52162
Elements	43598	109021	108542	505029	152172	160388

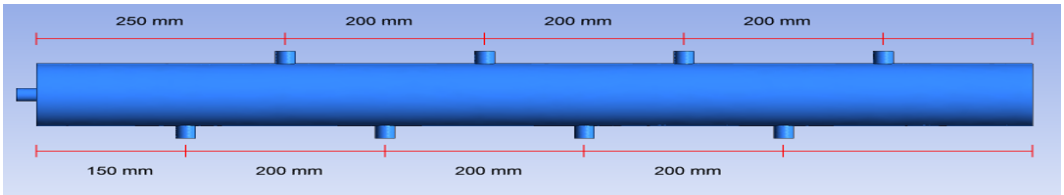

Figure 2.4 Case 3: Single end-wall port and an array of four pairs of staggered sidewall injection ports.

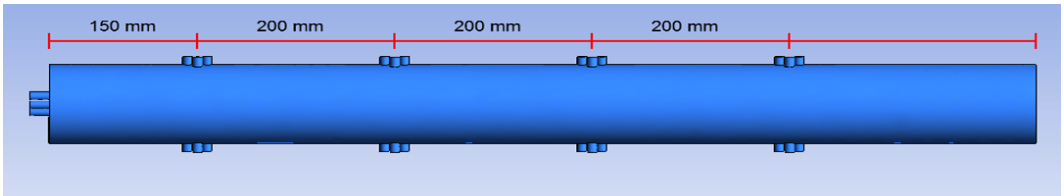

Figure 2.5 Case 4: Single end-wall port and array of four pairs of showerhead opposing sidewall ports.

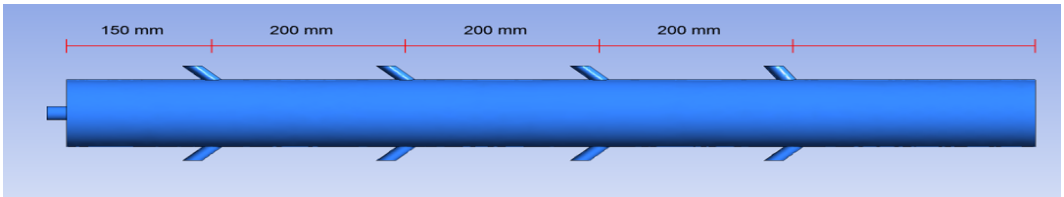

Figure 2.6 Case 5: Sidewall injection with ports inclined 45 deg downstream.

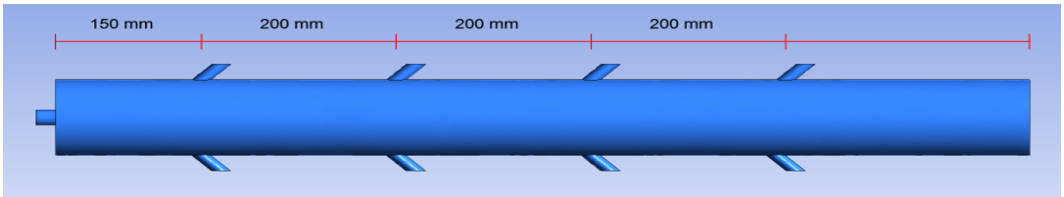

Figure 2.7 Case 6: Sidewall injection with ports inclined 45 deg upstream.

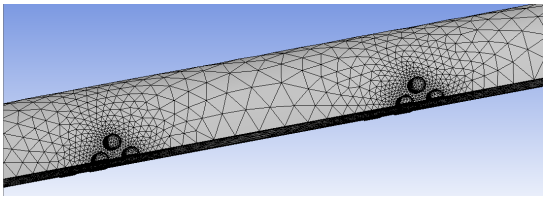

Figure 2.8 Meshing model for Case 4: showerhead sidewall injection.

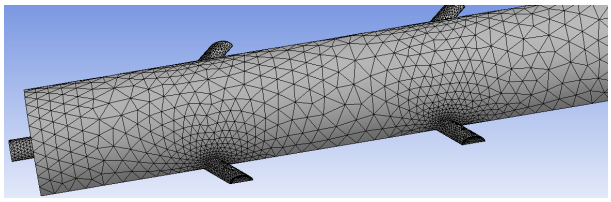

Figure 2.9 Meshing model for Case 6: angled upstream sidewall injection.

2.1.3 Analysis

ANSYS FLUENT was used to numerically solve the Reynolds-averaged Navier–Stokes equations with a realizable k-ϵ turbulence model with standard wall functions for surfaces on the mesh created by ANSYS MESHING and with a transient flow model. The mixture model was pressure-based at STP. The Volume of Fluid (VoF) multiphase model was used for the two phases, namely, air initially filling the tube and the gaseous octane/air mixture that was introduced. The volume fraction of the propellant mixture was monitored by the VoF model. For reliable simulations, a 0.01 ms time step size was chosen by trial-and-error for all the six cases.

2.1.3.1 Simultaneous Injection for the Six Cases

This simple methodology injects the propellant mixture from each port simultaneously at an equal rate. The static pressure of the propellants was kept at 1 atm, the same as in the tube. Three flow velocities for all these cases were chosen to be 40, 150 and 250 m/s.

2.1.3.2 Phased Injection

This method was used in an attempt to speed up the filling of the tube while reducing the amount of propellant exhausting from it. The phase delay was 15 ms for the 40 m/s injection rate, 10 ms for the 150 m/s injection rate and 5 ms for the

250 m/s injection rate. Only a selected number of configurations were chosen for this study.

CHAPTER 3

RESULTS AND DISCUSSION

3.1 Convergence

Convergence was determined when the residuals of t hecontinuity, component velocity, epsilon and k values become less than 0.001. Each time step was limited to a maximum of 1,000 iterations which was more than adequater for ensuring convergence. The total simulation time frame was set to 0.5 s which means that each run requires 50,000 time steps with the results monitored every 100 time steps or 1 ms. FLUENT automatically proceeds to next time step when the solution is converged and updates the data of every monitored parameter.

3.2 Simultaneous Injection at 40 m/s

3.2.1 Case 1

As shown in the contour plots of the volume fraction in Fig. 3.1, the gaseous propellant mixture slowly propagates from the single end wall injection toward the tube outlet. At the end of the entire time frame of calculation of 0.5 s, the mixture has not even reached the outlet, showing clearly the poor performance of this configuration with this injection rate. A criterion was set for the volume fraction to reach 0.9 as a satisfactory fill. However, at 0.5 s, the volume fraction that was achieved was only 0.4, far below the requirement.

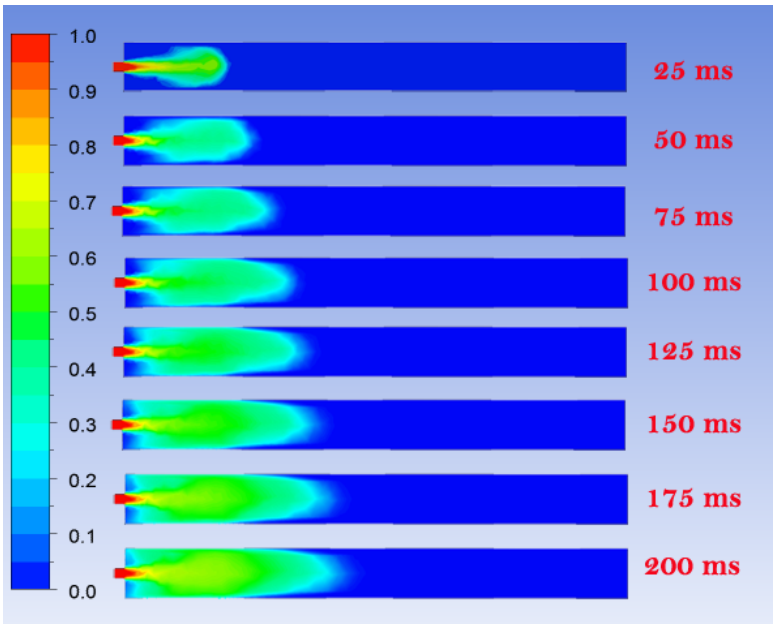

Figure 3.1 Case 1: Contour of volume fraction of mixture at injection rate of 40 m/s.

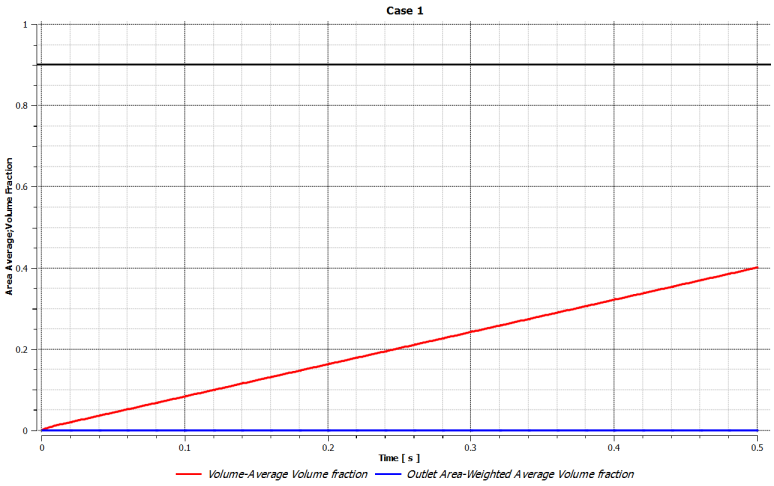

Figure 3.2 Case 1: Volume fraction and exit concentration at 40 m/s.

3.2.2 Case 2

The addition of four pairs of sidewall ports increased the overall flowrate from Case 1 by ninefold and this is reflected by the more rapid filling as shown in Fig. 3.4. Around 150 ms, the volume fraction has reached 80–90 percent, Fig. 3.5. The

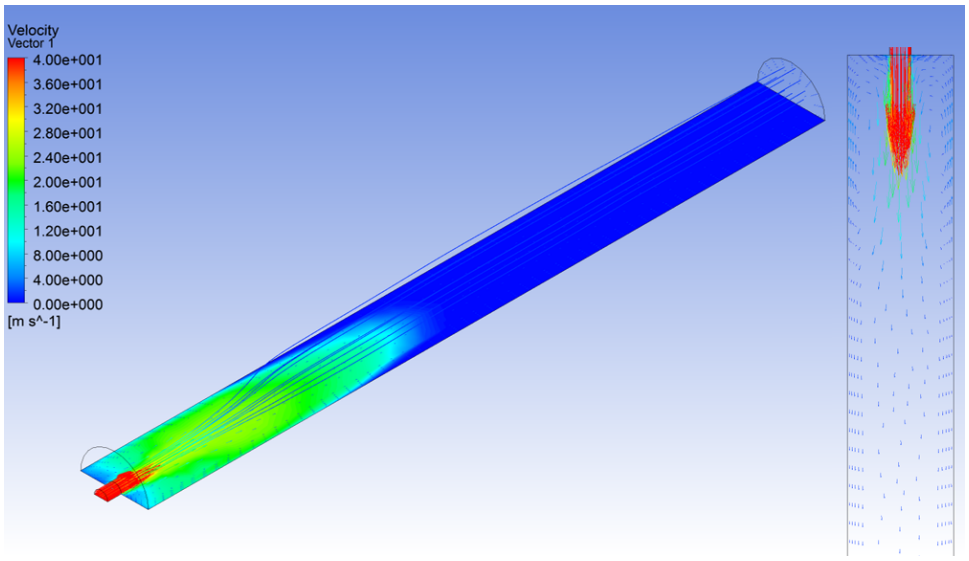

Figure 3.3 Case 1: Velocity vectors, streamlines and concentrations at 200 ms.

concentration at the exit plane follows the volume fraction with a slight delay. This case revealed the presence of a dead region near the closed end.

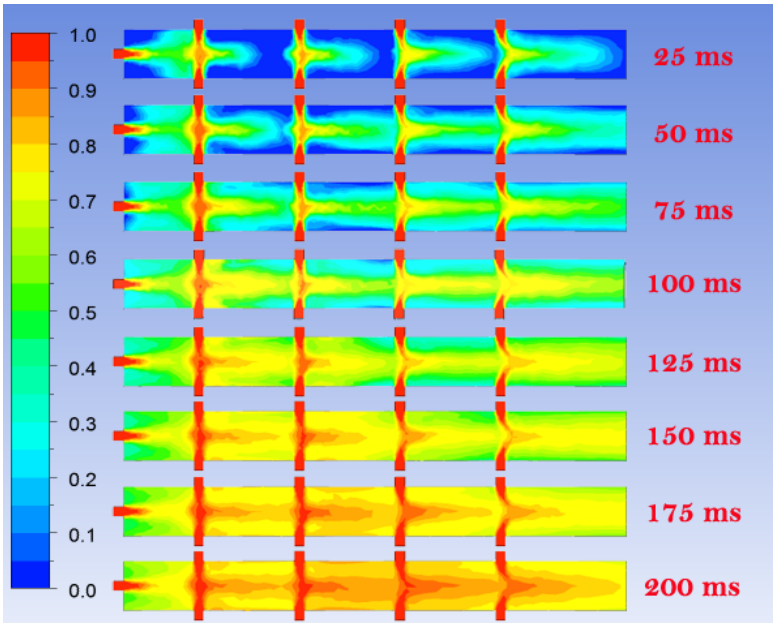

Figure 3.4 Case 2: Contour of volume fraction of mixture at injection rate of 40 m/s.

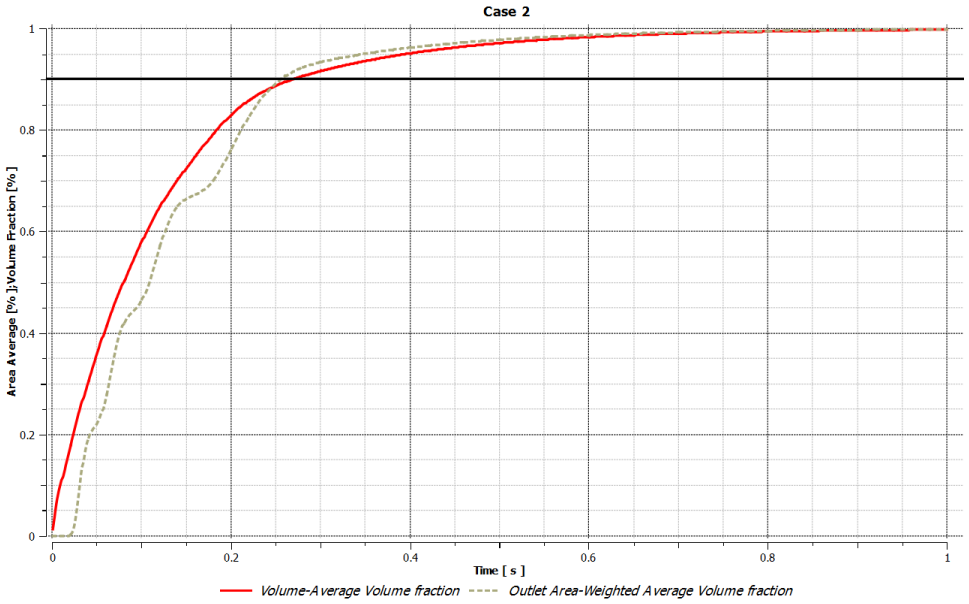

Figure 3.5 Case 2: Volume fraction and exit concentration at 40 m/s.

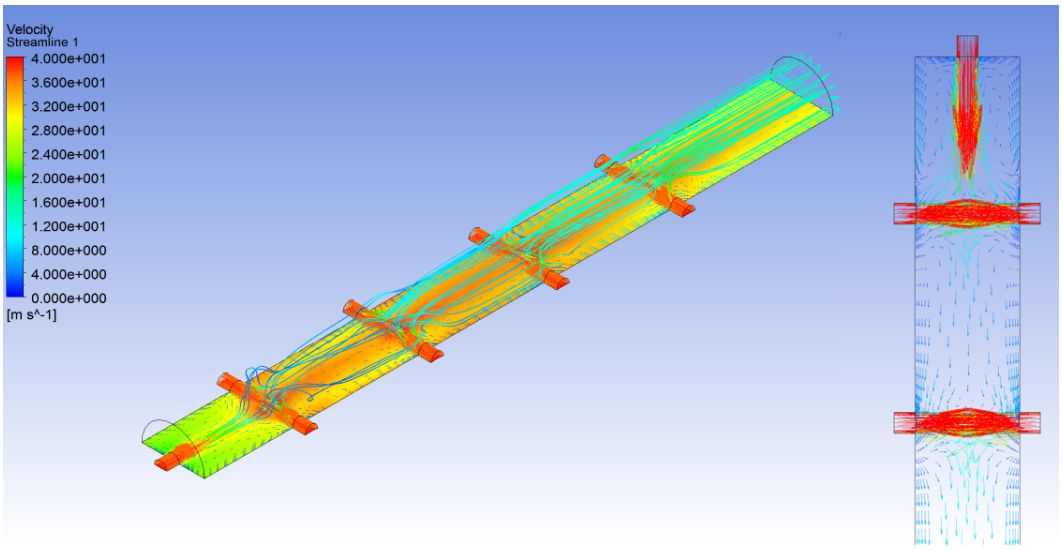

Figure 3.6 Case 2: Velocity vectors, streamlines and concentrations at 200 ms.

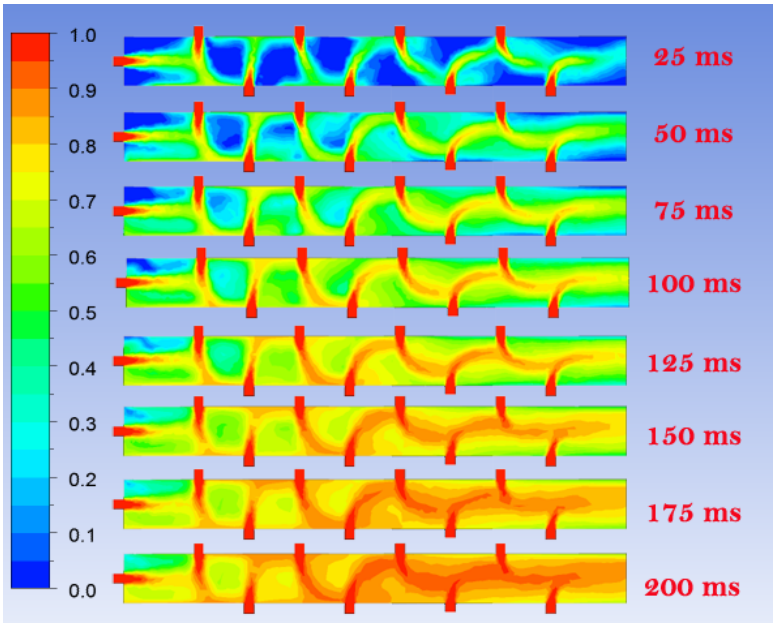

Figure 3.7 Case 3: Contour of volume fraction of mixture at injection rate of 40 m/s.

3.2.3 Case 3

This configuration was designed for removing the dead regions due to the partial blockage produced by the opposing jets. However, as can be seen in Fig. 3.7, this configuration was not successful. In fact, it produced large dead regions between each staggered port and did not remove the dead region near the end wall. As can be seen in Fig. 3.8, the 90 percent volume fraction requirement now took almost 330 ms, much longer than for Case 2.

3.2.4 Case 4

Figures 3.10 and 3.11 indicate a rapid initial fill but the rate of increase of the volume fraction slowed down after 0.1 ms. The fill took about 410 ms to reach a volume fraction of 90 percent.

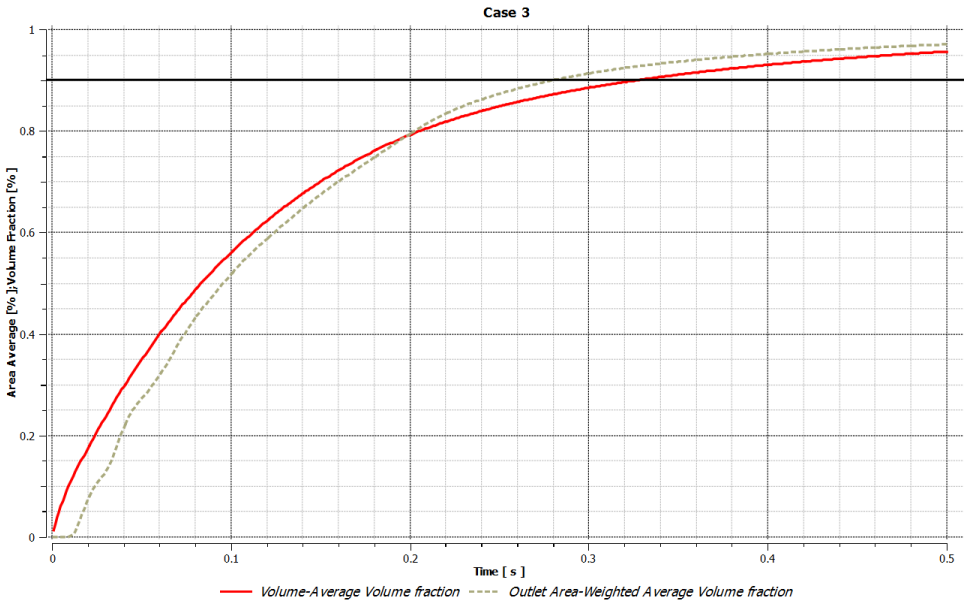

Figure 3.8 Case 3: Volume fraction and exit concentration at 40 m/s.

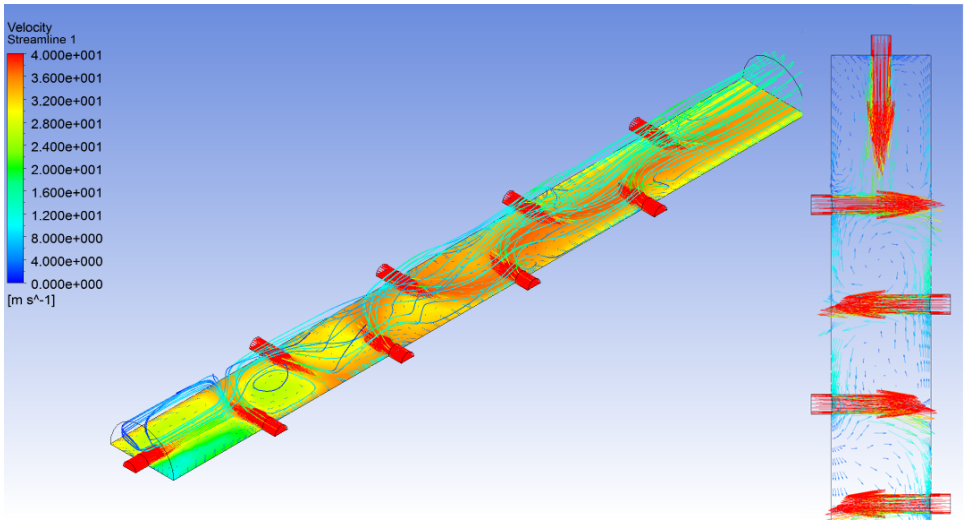

Figure 3.9 Case 3: Velocity vectors, streamlines and concentrations at 200 ms .

3.2.5 Case 5

Figures 3.13 and 3.14 show that there is excessive loss of propellant and that it took almost 440 ms for the 90 percent volume fraction criterion to be met. Figure 3.15

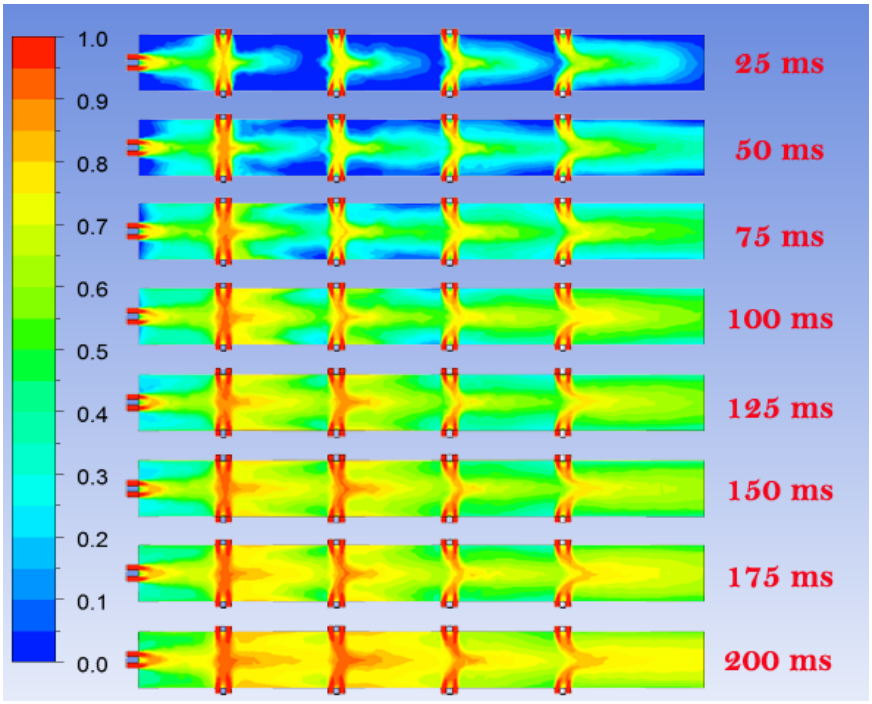

Figure 3.10 Case 4: Contour of volume fraction of mixture at injection rate of 40 m/s.

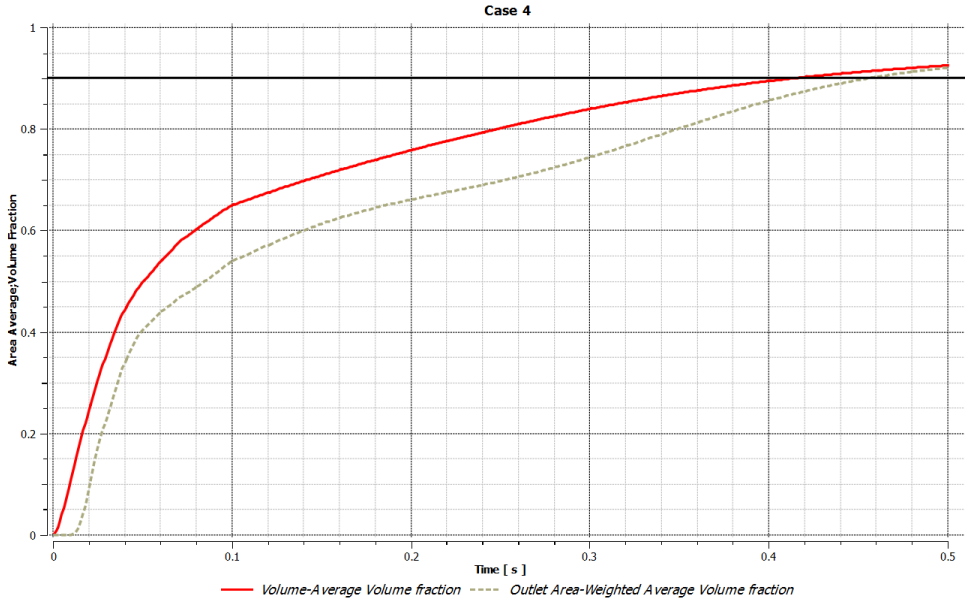

Figure 3.11 Case 4: Volume fraction and exit concentration at 40 m/s.

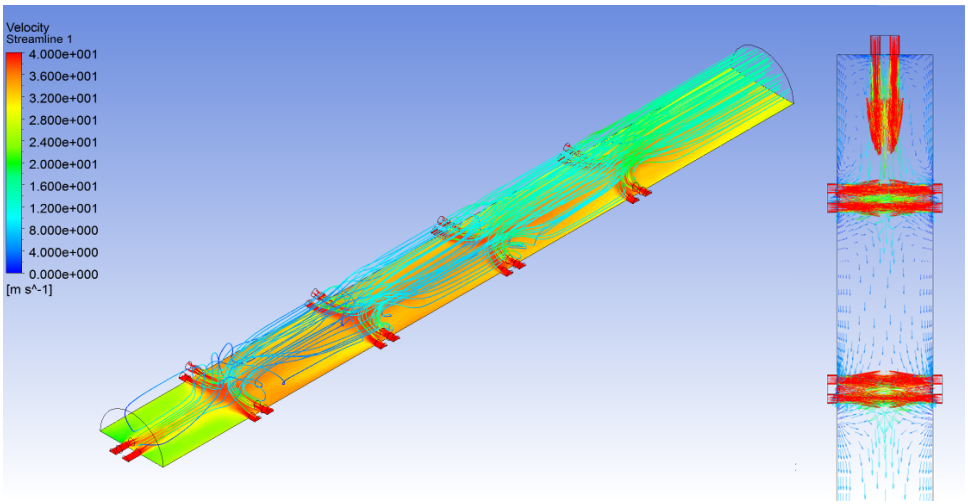

Figure 3.12 Case 4: Velocity vectors, streamlines and concentrations at 200 ms.

shows clearly that the downstream facing injection ports rapidly filled the downstream region at the expense of a poorly filled region near to the endwall.

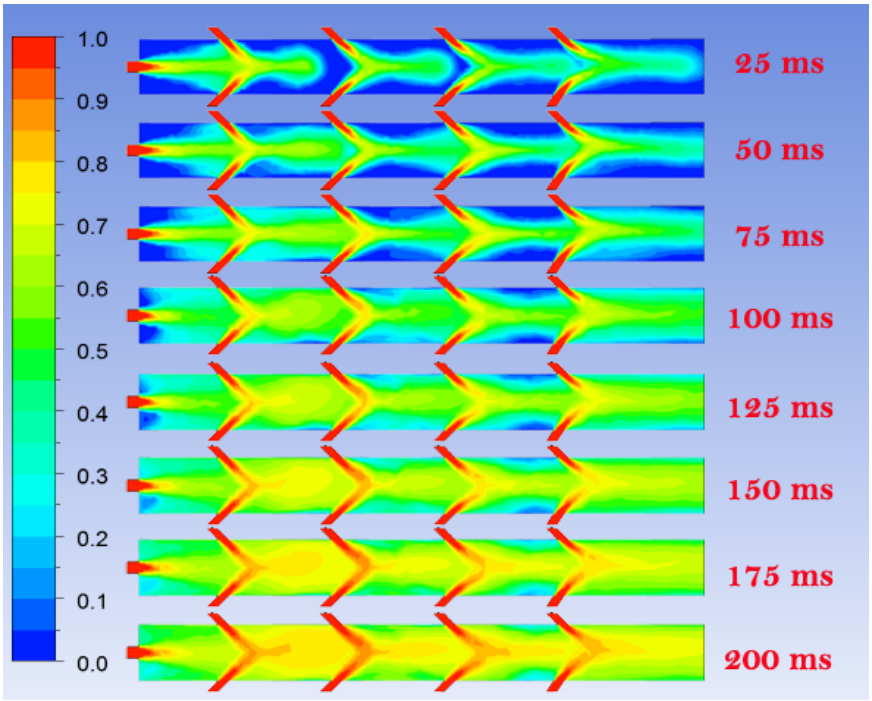

Figure 3.13 Case 5: Contour of volume fraction of mixture at injection rate of 40 m/s.

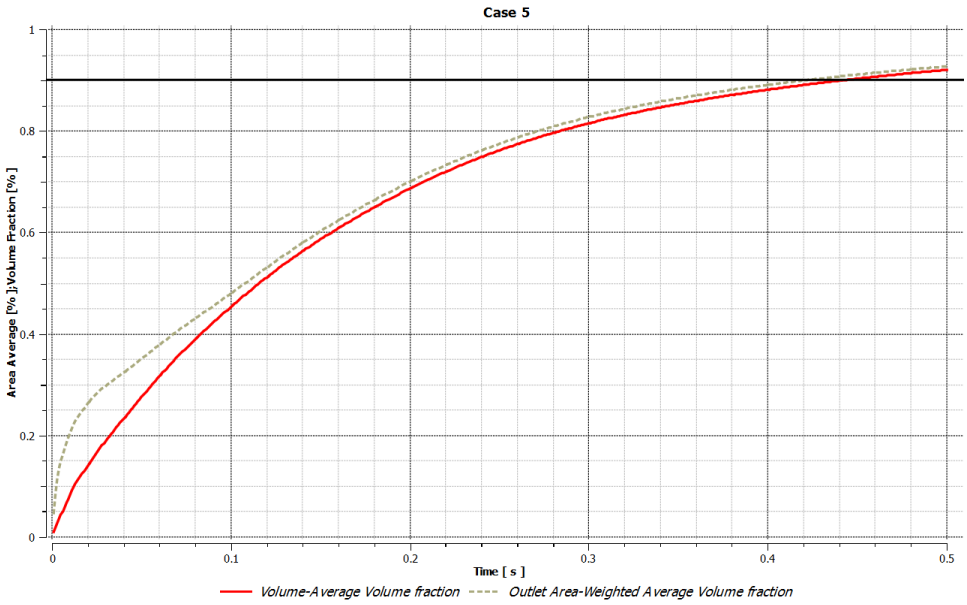

Figure 3.14 Case 5: Volume fraction and exit concentration at 40 m/s.

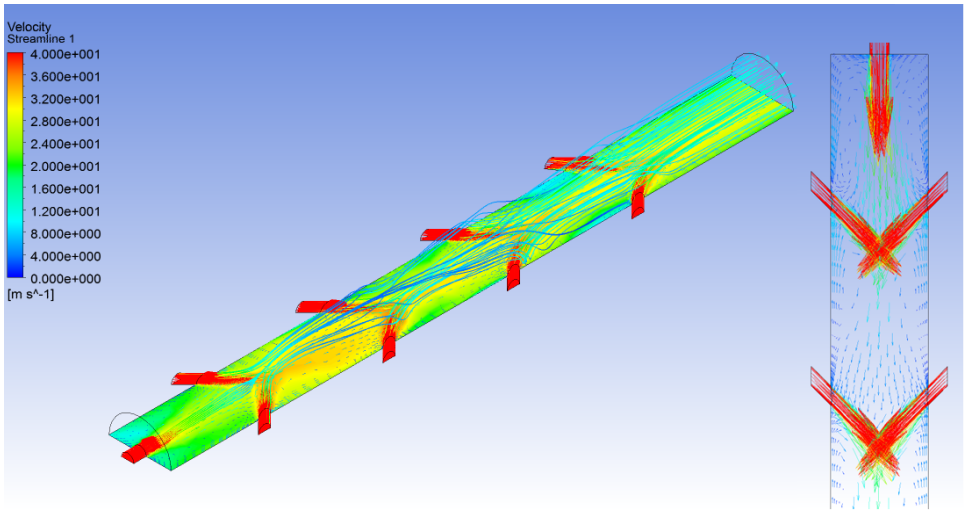

Figure 3.15 Case 5: Velocity vectors, streamlines and concentrations at 200 ms.

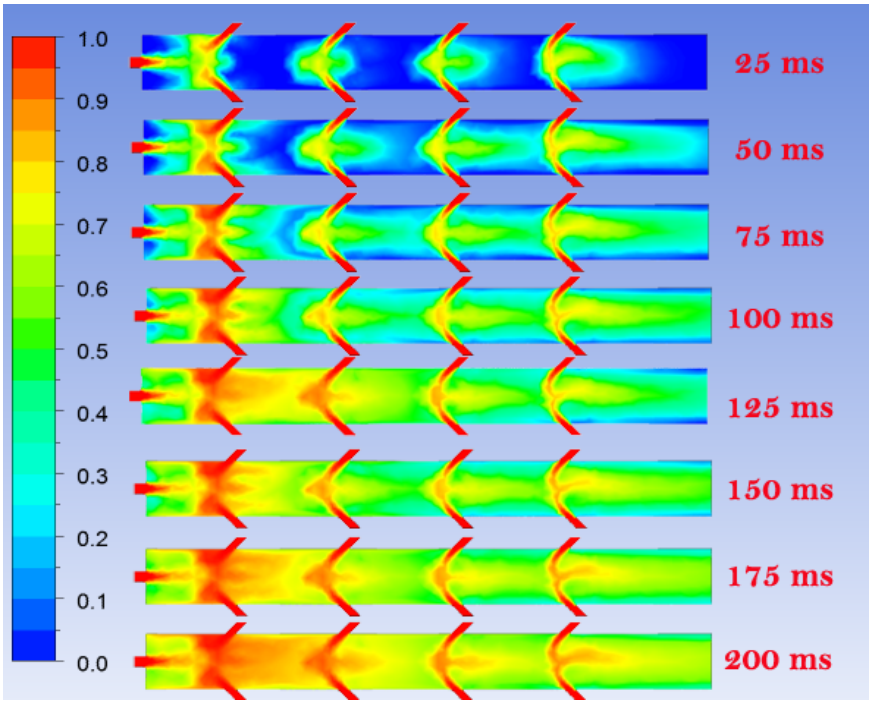

Figure 3.16 Case 6: Contour of volume fraction of mixture at injection rate of 40 m/s.

3.2.6 Case 6

Due to the poor performance of Case 5, ports inclined upstream were considered here. This case was thought to be able to raise the propellant concentration rapidly especially around the endwall. Figure 3.16 shows that this was achieved with a high concentration of propellant at the vicinity of the endwall and the first pair of injection ports. Nevertheless for the entire volume, it took 280 ms to reach 90 percent fill, a little slower than Case 2, Fig. 3.17. The reasons for this are the presence of a small dead region near the endwall and the low concentration further downstream especially away from the centerline; see also Fig. 3.18.

Figure 3.19 summarizes the volume fraction and the exit concentration for all six cases. It can be seen that despite Case 1 being referred to as the baseline configuration, the single port is obviously inadequate compared to the total flow afforded by seven

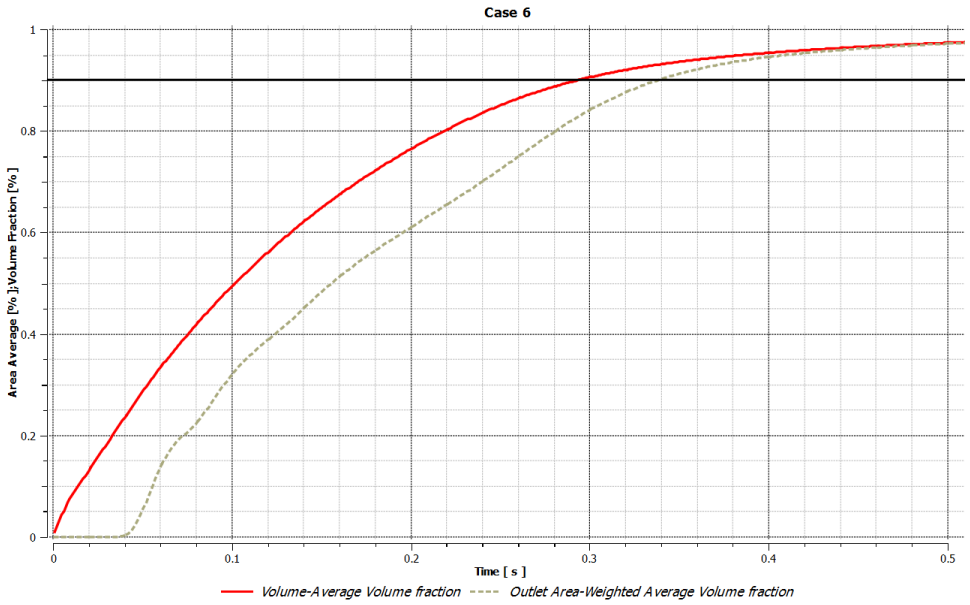

Figure 3.17 Case 6: Volume fraction and exit concentration at 40 m/s.

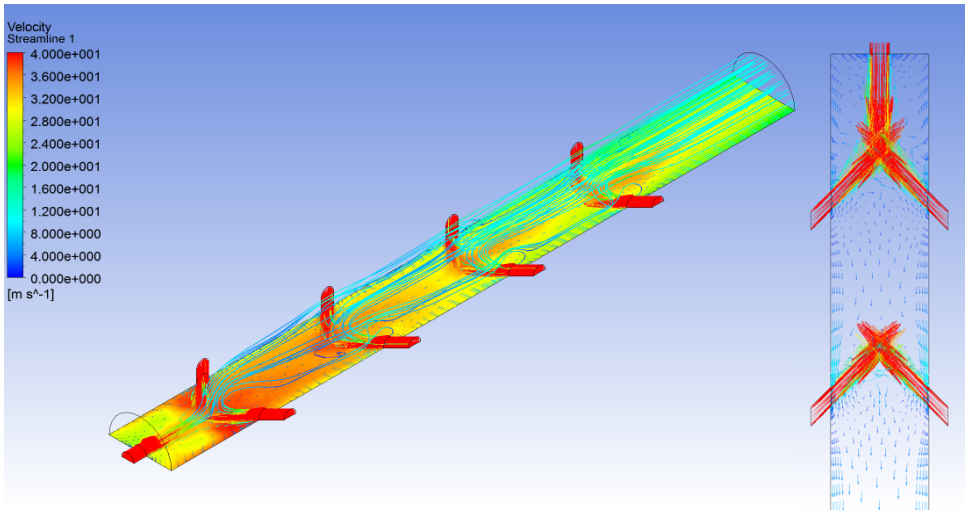

Figure 3.18 Case 6: Velocity vectors, streamlines and concentrations at 200 ms.

ports. The summary plot shows that case 4 showed outstanding fill capability before 100 ms but slowed after that. Case 2, the opposing, normal sidewall injection case, is the first configuration to reach 90 percent fill, followed by case 6, the upstream-facing

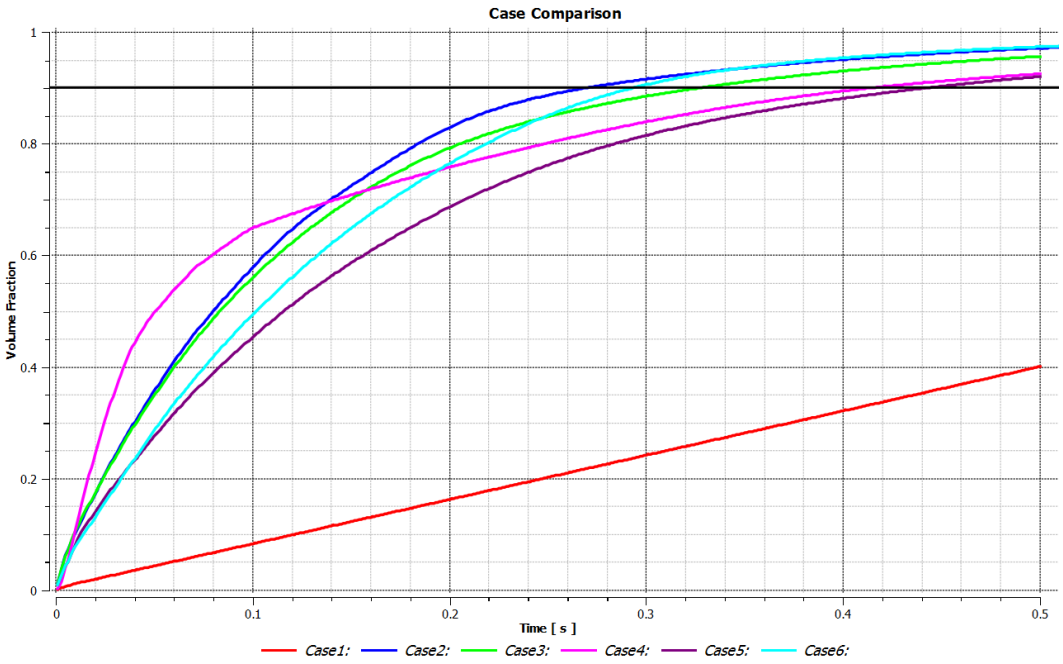

Figure 3.19 Summary of volume fraction for all cases at an injection rate of 40 m/s .

injection configuration, and case 3, the staggered sidewall configuration. Case 4 and Case 5 were the slowest, discounting Case 1.

3.3 Simultaneous Injection at an Increased Rate of 150 and 250 m/s

Due to the poor overall results at an injection rate of 40 m/s, the next step was to increase the injection rate. Rates that were chosen were 150 and 250 m/s for all cases, less Case 1. The concentration contours for fill rates of 150 m/s at chosen time steps are shown below in Figs. 3.20– 3.24. Due to the increased flow, all these cases showed a more rapid fill. Case 2 still was the first to reach 90 percent volume fraction, followed by Case 6, the upstream injection configuration. Case 6 showed a slow rise in volume fraction initially but subsequently increased rapidly compared to the other cases. Case 3 shows a middle performance and Case 4, the showerhead, is now the slowest.

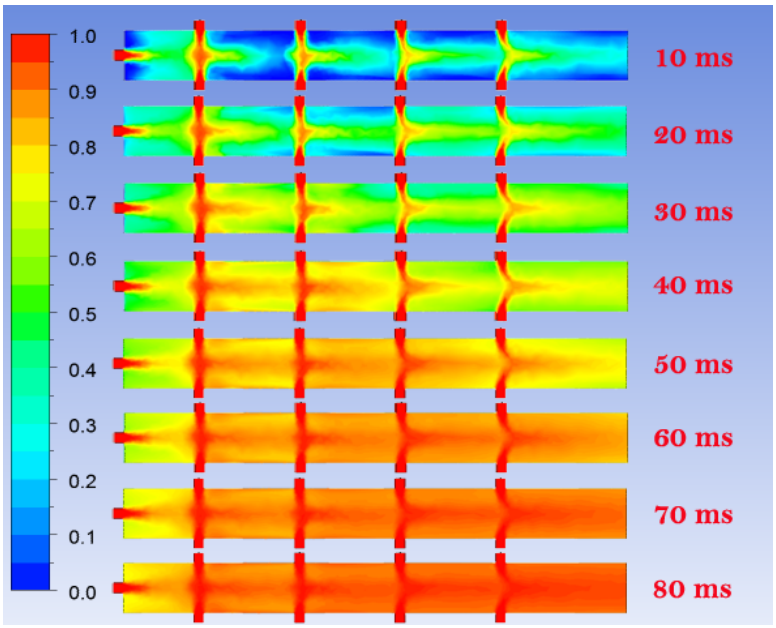

Figure 3.20 Case 2: Contour of volume fraction of mixture at injection rate of 150 m/s.

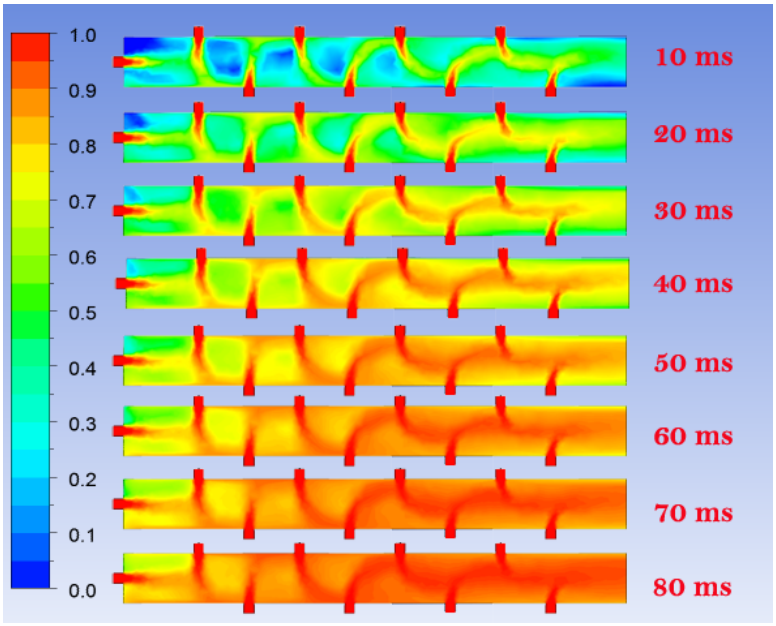

Figure 3.21 Case 3: Contour of volume fraction of mixture at injection rate of 150 m/s.

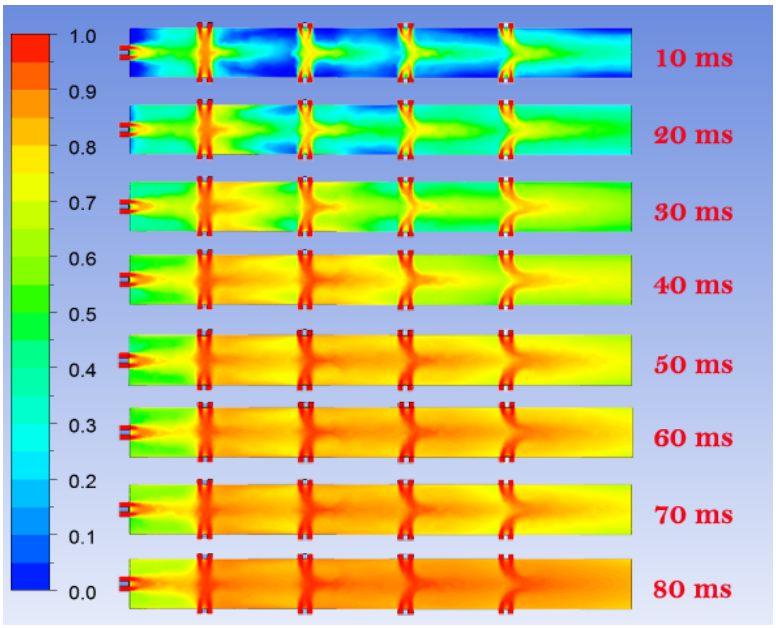

Figure 3.22 Case 4: Contour of volume fraction of mixture at injection rate of 150 m/s.

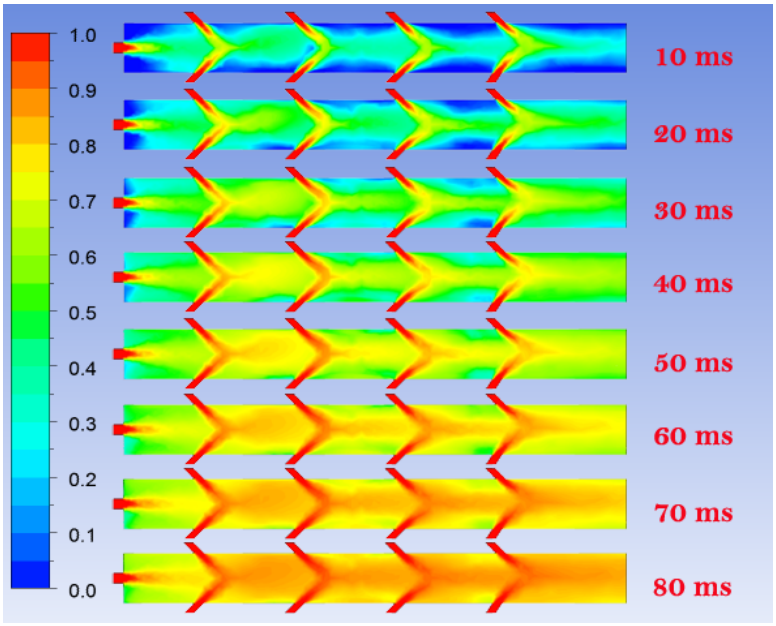

Figure 3.23 Case 5: Contour of volume fraction of mixture at injection rate of 150 m/s.

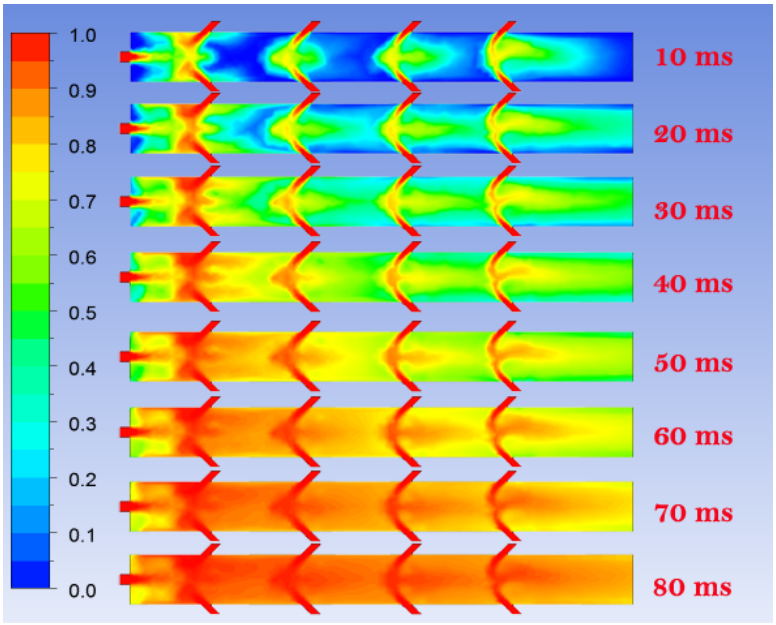

Figure 3.24 Case 6: Contour of volume fraction of mixture at injection rate of 150 m/s.

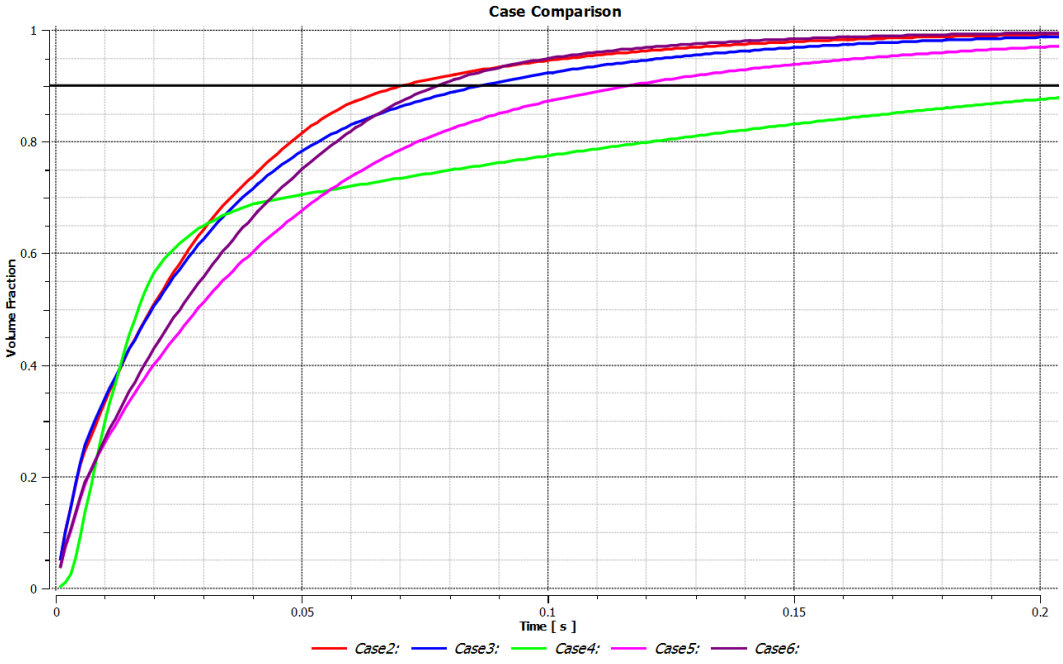

Figure 3.25 Summary of volume fraction for Cases 2-6 at an injection rate of 150 m/s.

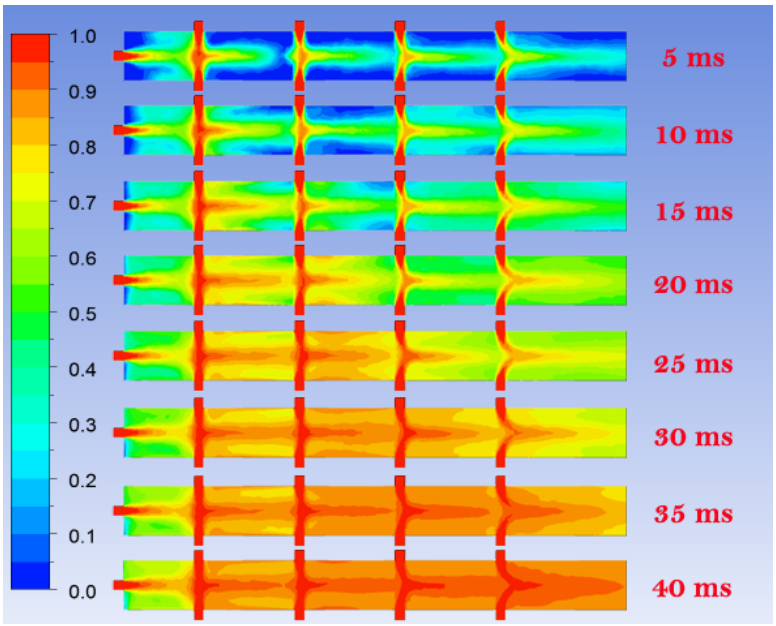

Figure 3.26 Case 2: Contour of volume fraction of mixture at injection rate of 250 m/s.

At an injection rate of 150 m/s, cases 2 and 6 showed that they can achieve 90 percent volume fraction at 70 and 76 ms respectively. Due to their excellent performance, these two cases were selected to have the injection rate raised to 250 m/s. The contour plots of the volume fraction for these two cases are shown in Figs. 3.26 and 3.26 respectively. FIgure 3.28 shows the marked improvement in performance, with both configurations capable of filling the tube to 90 percent volume fraction in under 50 ms. Nonetheless, even this fill rate is unable to satisfy the posed requirement.

3.4 Phased Injection

The final strategy to increase tube performance is phased injection. Only Cases 2 and 6 were selected with injection rates of 150 and 250 m/s. The phased delay was 10 ms for the former and 5 ms for the latter injection rate, after the endwall port was opened, sequentially from the most upstream pair toward the downstream. The

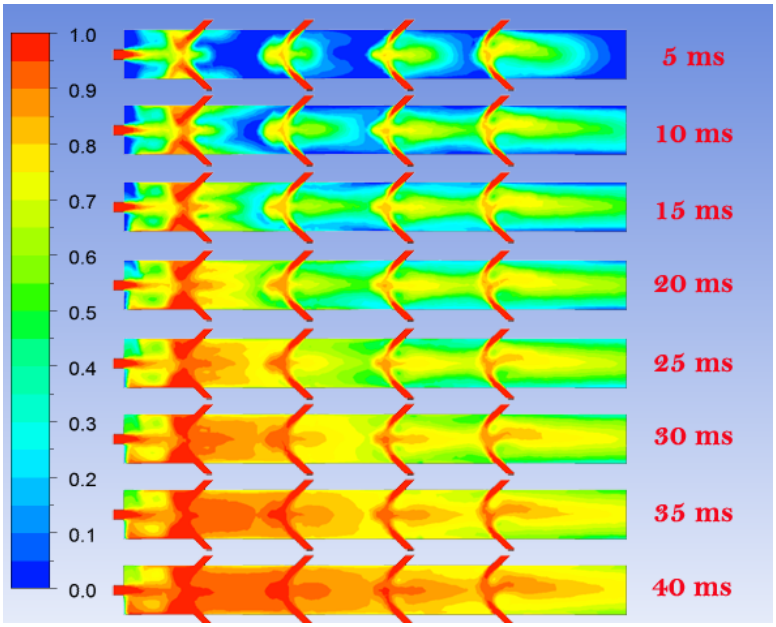

Figure 3.27 Case 6: Contour of volume fraction of mixture at injection rate of 250 m/s.

concentration contours for the 150 m/s injection rate for Cases 2 and 6 are shown in Figs. 3.29 and 3.30. The performance is summarized in Fig. 3.31 which shows that both reached 90 percent volume fraction at almost the same time at 77 ms. The concentration at the exit starts to become evident after the last pair of injection ports was opened. The exit concentration remained zero until amost 50 ms after the process started.

Finally, the phased injection rate was increased to 250 m/s with a 5 ms delay. The concentration contours are shown in Figs. 3.32 and 3.33. Both cases reached the 90 percent volume fraction requirement in about 47 ms. Finally, Fig. 3.34 shows that the concentration at the exit is delayed for Case 6 to almost 30 ms, which is longer than Case 2 by about 5 ms. This delay is a desired outcome.

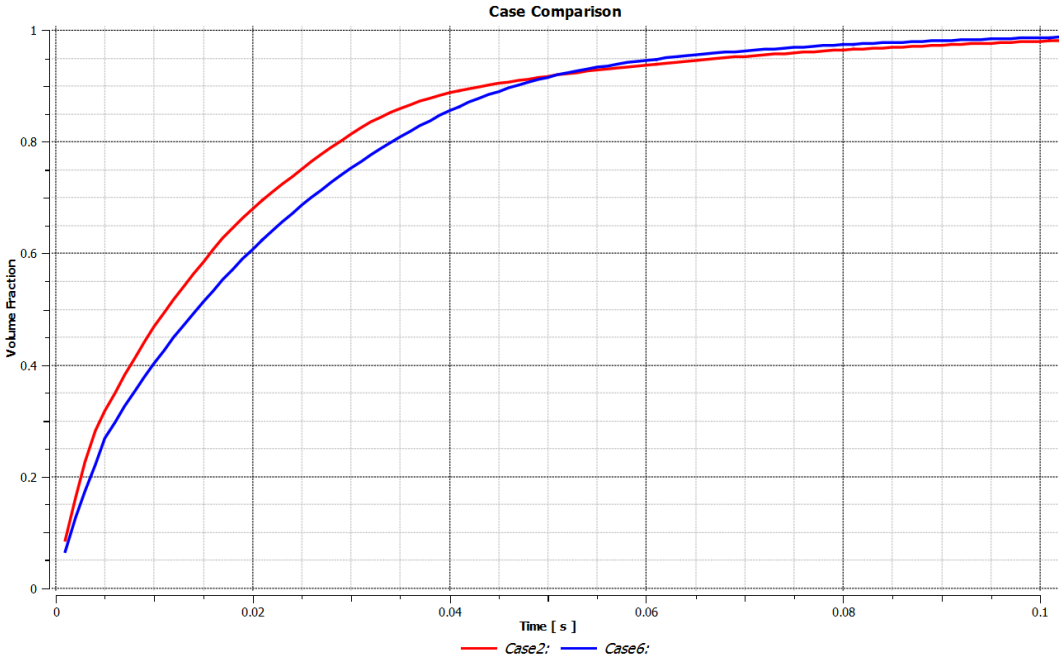

Figure 3.28 Summary of volume fraction for Cases 2 and 6 at an injection rate of 250 m/s.

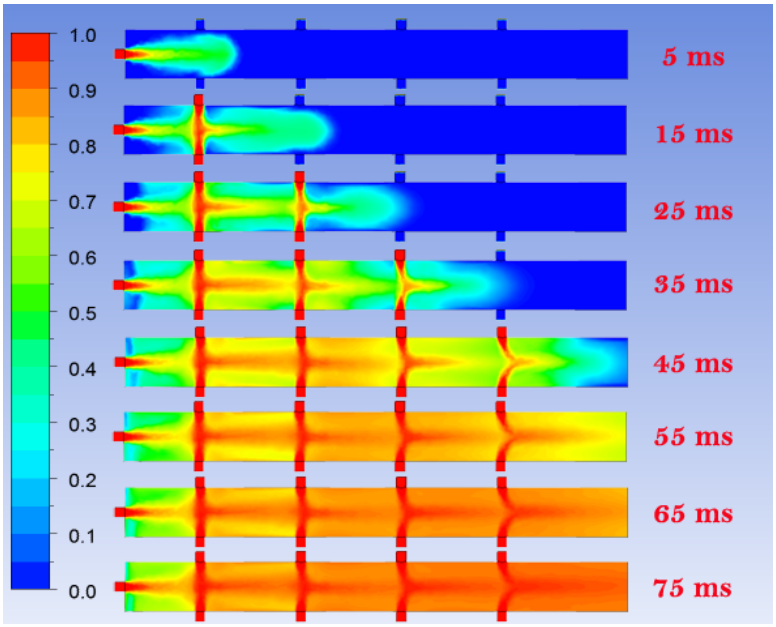

Figure 3.29 Case 2: Contour of volume fraction of mixture at injection rate of 150 m/s with a 10 ms sequential phased delay from endwall to the most downstream pairs of ports.

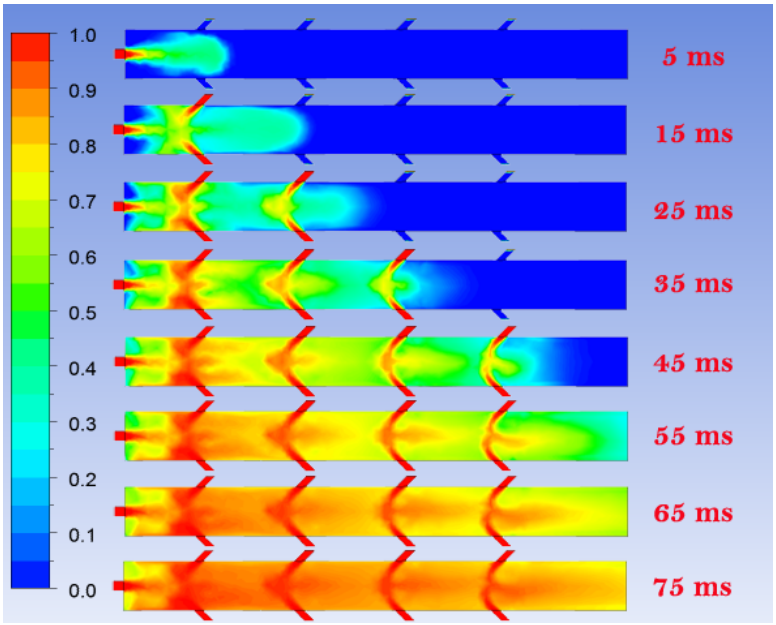

Figure 3.30 Case 6: Contour of volume fraction of mixture at injection rate of 150 m/s with a 10 ms sequential phased delay from endwall to the most downstream pairs of ports.

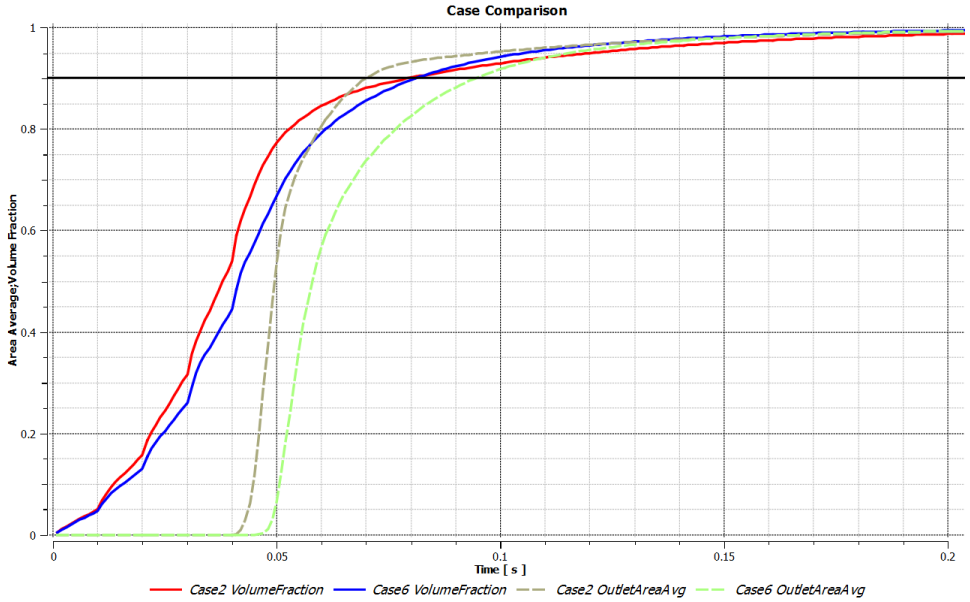

Figure 3.31 Summary of phased injection at 150 m/s and time delay of 10 ms showing volume fraction and exit concentration.

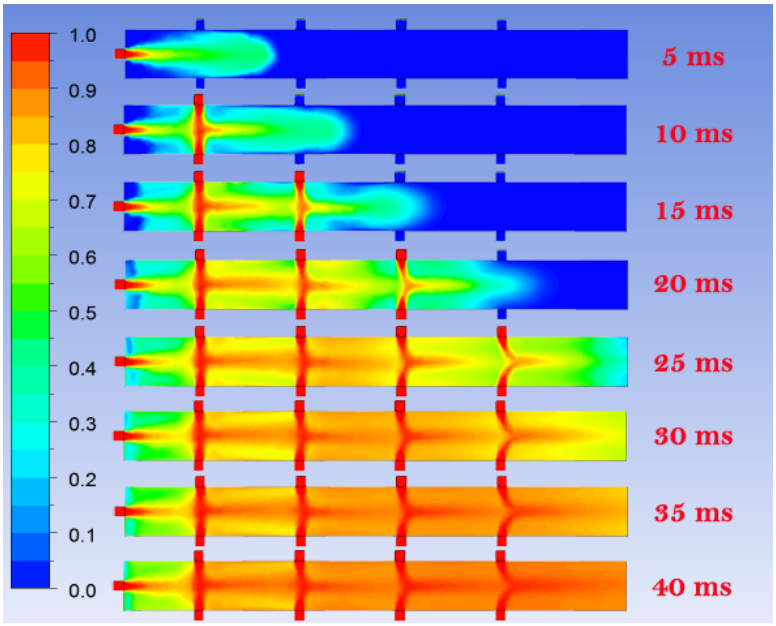

Figure 3.32 Case 2: Contour of volume fraction of mixture at injection rate of 250 m/s with a 5 ms sequential phased delay from endwall to the most downstream pairs of ports.

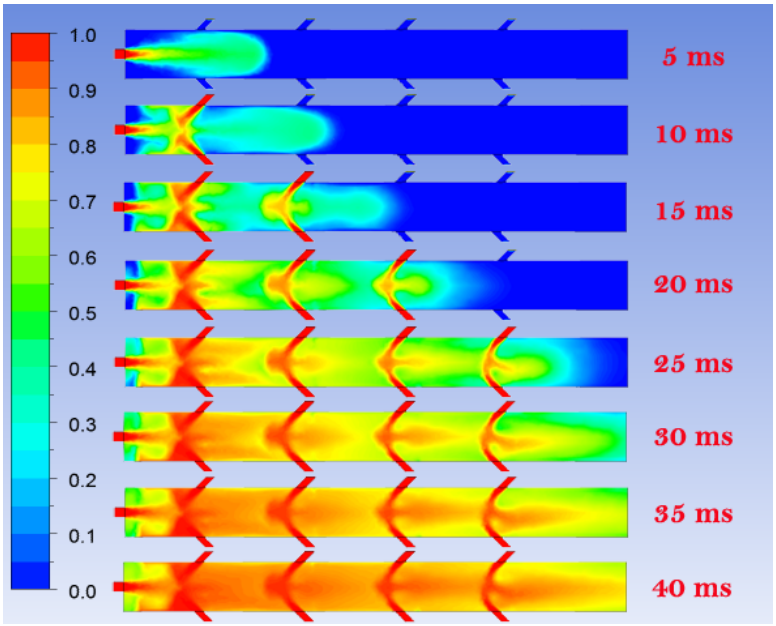

Figure 3.33 Case 6: Contour of volume fraction of mixture at injection rate of 250 m/s with a 5 ms sequential phased delay from endwall to the most downstream pairs of ports.

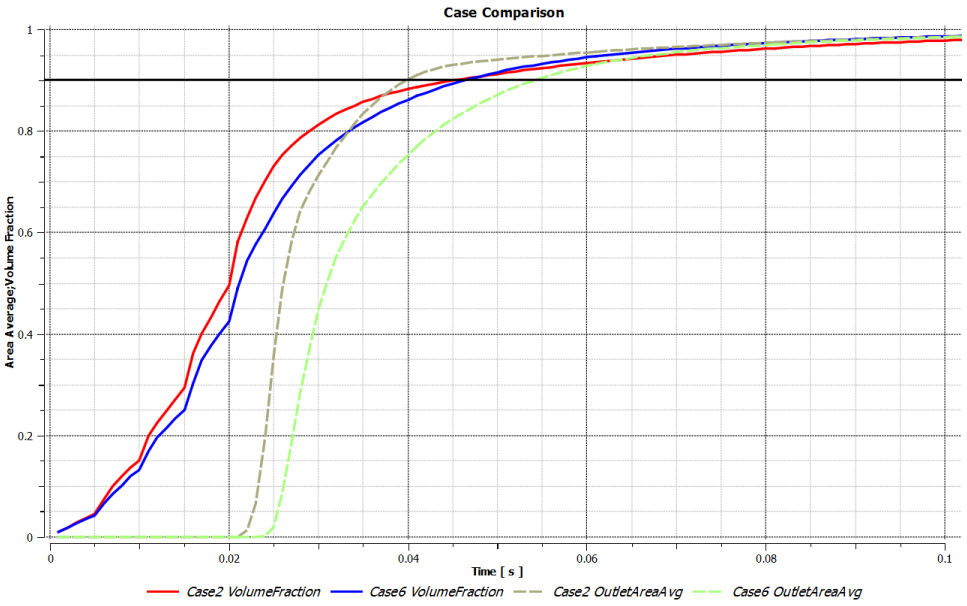

Figure 3.34 Summary of phased injection at 250 m/s and time delay of 5 ms showing volume fraction and exit concentration.

CHAPTER 4

CONCLUSION AND RECOMMENDATIONS FOR FUTURE WORK

4.1 Conclusion

Six different injection configurations were examined in this study, from a simple configuration with one endwall injection to phased injection at high rates. The highest injection rate of 250 m/s with upstream facing injectors appear to produce the best performance but were still unable to fulfill the 10 ms requirement.

4.2 Recommendations For Future Work

This study shows that none of the filling strategies can fulfill the 10 ms requirement. A further increase in injection rate and an increase in fill pressure to produce supersonic filling should be considered. Larger ports should also be considered. Due to the overall improvement of the upstream, phased injection case (Case 6), further attention should be placed to implementing these recommendations with this configuration.

REFERENCES

[1] R. Vutthivithayarak, E. M. Braun, and F. K. Lu, "Examination of the various cycles for pulse detonation engines," *AIAA Paper 2011-6064*, 2011.

[2] T. Bussing and G. Pappas, "An introduction to pulse detonation engines," *AIAA Paper 94-0263*, 1994.

[3] K. Kailasanath, "Recent developments on the research on pulse detonation engines," *AIAA Journal*, vol. 41(2), pp. 145–159, 2003.

[4] S. M. Frolov, V. Y. Basevich, V. S. Aksenov, and S. A. Polikhov, "Liquid-fueled, air-breathing pulse detonation engine demonstrator: Operation principles and performance," *Journal of Propulsion and Power*, vol. 22(6), pp. 1162–1169, 2006.

[5] J. L. Li, W. Fan, C. J. Yan, and Q. Li, "Experimental investigations on detonation initiation in a kerosene-oxygen pulse detonation rocket engine," *Combustion Science and Technology*, vol. 181(3), pp. 417–432, 2009.

BIOGRAPHICAL STATEMENT

Wunnarat Rongrat was born and lived his early life in Bangkok, Thailand. He completed his Bachelors degree in Aeronautical Engineering from the Royal Thai Air Force Academy. After that he was an engineer with the Directorate of Aeronautical Engineering, working with aircraft weight balance and accident investigation. His interest in computer engineering and programming brought him to attend an ANSYS FLUENT tutorial course by ANSYS, Inc. This led to the great outcome in his contribution in Dr. Frank K. Lu's research group.